

An adaptive delay compensation method based on a discrete system model for real-time hybrid simulation

Zhen Wang^{1,2,3,4a}, Guoshan Xu^{*2,3,4}, Qiang Li^{2,3,4} and Bin Wu^{1b}

¹ School of Civil Engineering and Architecture, Wuhan University of Technology, Wuhan 430070, China

² Key Lab of Structures Dynamic Behavior and Control of the Ministry of Education, Harbin Institute of Technology, Harbin 150090, China

³ Key Lab of Smart Prevention and Mitigation of Civil Engineering Disasters of the Ministry of Industry and Information Technology, Harbin Institute of Technology, Harbin 150090, China

⁴ School of Civil Engineering, Harbin Institute of Technology, Harbin 150090, China

(Received July 19, 2019, Revised November 13, 2019, Accepted December 17, 2019)

Abstract. The identification of delays and delay compensation are critical problems in real-time hybrid simulations (RTHS). Conventional delay compensation methods are mostly based on the assumption of a constant delay. However, the system delay may vary during tests owing to the nonlinearity of the loading system and/or the behavioral variations of the specimen. To address this issue, this study presents an adaptive delay compensation method based on a discrete model of the loading system. In particular, the parameters of this discrete model are identified and updated online with the least-squares method to represent a servo hydraulic loading system. Furthermore, based on this model, the system delays are compensated for by generating system commands using the desired displacements, achieved displacements, and previous displacement commands. This method is more general than the existing compensation methods because it can predict commands based on multiple displacement categories. Moreover, this method is straightforward and suitable for implementation on digital signal processing boards because it relies solely on the displacements rather than on velocity and/or acceleration data. The virtual and real RTHS results show that the studied method exhibits satisfactory estimation smoothness and compensation accuracy. Furthermore, considering the measurement noise, the low-order parameter models of this method are more favorable than that the high-order parameter models.

Keywords: real-time hybrid simulation; delay compensation; adaptive compensation; discrete model

1. Introduction

Since proposed in 1992 (Nakashima *et al.* 1992), real-time hybrid simulations (RTHS) have been drawing increasing attention and have been extensively investigated (Horiuchi *et al.* 1999, Ahmadzadeh *et al.* 2008, Gao *et al.* 2013, Ou *et al.* 2015, Wang *et al.* 2016, Chae *et al.* 2017, Eem *et al.* 2018, Zhang *et al.* 2019). Applications of this technique for performance evaluations of dynamic systems have been reported in recent years, including offshore platforms, wood buildings, steel-frame structures, wind turbines, and other vibration-controlled structures (Christenson and Lin 2008, Wu *et al.* 2011, Chae *et al.* 2014, Shao *et al.* 2014, Zhang *et al.* 2019, Chen *et al.* 2019, Lu *et al.* 2019). This technique separates the emulated systems into a numerical substructure (NS) and physical substructure (PS). The NS often refers to the part numerically modeled and simulated, and the PS represents the part physically fabricated and tested in laboratories. The PS is often unsuitable for conducting numerical analysis owing to its complex and/or rate-dependent behaviors. This

technique takes advantage of numerical simulations and physical experiments and achieves versatile performance in terms of a short testing period, low specimen and setup costs, and accurate testing results.

The delay and the corresponding compensation play significant roles in obtaining reliable test results in RTHS. The delay in an RTHS mainly originates from the dynamics of the loading system adopted to ensure the boundary conditions between the PS and NS. Research has revealed that the delay may cause inaccuracy and instability problems in some cases, e.g., an RTHS with a spring specimen (Horiuchi *et al.* 1999, Wallace *et al.* 2005a, Wang *et al.* 2014, Huang *et al.* 2019).

Several delay compensation schemes are currently available. The most extensively used schemes are prediction schemes based on constant delay assumptions, including the polynomial extrapolation method (Horiuchi *et al.* 1999, Nakashima *et al.* 1999, Darby *et al.* 2002, Ning *et al.* 2019) and kinematic predictors (Horiuchi and Konno 2001, Ahmadzadeh *et al.* 2008). In essence, delay compensation substantially reduces the phase lag of the loading system. Hence, several control schemes have been employed to achieve this objective, such as the phase-lead network (Zhao *et al.* 2003), feedforward control (Jung and Shing 2006), inverse control (Chen and Ricles 2009), outer loop control (Bonnet *et al.* 2007), model-based feedforward-feedback control (Phillips and Spencer 2013), optimal discrete-time feedforward control (Hayati and Song 2017),

*Corresponding author, Associate Professor,
E-mail: xuguoshan@hit.edu.cn

^a Ph.D., E-mail: zhenwang@hit.edu.cn

^b Professor, E-mail: bin.wu@hit.edu.cn

and sliding mode control (Wu and Zhou 2014). Moreover, delay compensation via force correction was also proposed and investigated (Ahmadizadeh *et al.* 2008, Wu *et al.* 2013).

In real tests, the system delay often varies owing to the nonlinearity of the loading system and the behavioral changes of the specimen. To accommodate delay variations, adaptive delay compensation methods were conceived. These methods achieved better performance than traditional schemes in terms of the compensation accuracy and adaptability in complex RTHS scenarios. One category of these methods is based on online delay estimation, where an online estimated delay is applied to traditional predictions for delay compensation (Darby *et al.* 2002, Ahmadizadeh *et al.* 2008, Wang *et al.* 2014). Another category adopts the strategy of inverse control, where the inverse model of a loading system is identified online (Chen *et al.* 2012, Chae *et al.* 2013). Additionally, adaptive compensation was performed based on the synchronization error and nonlinear estimator by Wallace *et al.* (2005b), Zhou *et al.* (2017), and Strano and Terzo (2016).

In contrast to the existing adaptive delay compensation methods, this study investigates a more general adaptive compensation method (Wang *et al.* 2018) based on a discrete model of the loading system in which the compensation commands of actuators are generated using the desired displacements, measured displacements, and previous displacement commands. It is notable that this method is different from that proposed by Ning *et al.* (2019), where the loading system delay was resolved by the traditional polynomial extrapolation and robust control strategy. The remainder of this study is organized as follows. Section 2 presents an overview of this adaptive delay compensation method. A virtual RTHS used for the examination of the performance of this method is described in Section 3. Section 4 presents the results of RTHS using the studied method. Section 5 summarizes the conclusions of this research study.

2. An overview of adaptive delay compensation method based on a discrete model

This section describes in detail the abovementioned adaptive delay compensation method (Wang *et al.* 2018), as shown in Fig. 1. Unlike delay compensation methods based on a continuous system model, this method models the

loading system with a discrete difference equation. This method first identifies and updates the parameters of the discrete model using actuator commands and displacement responses. Subsequently, these parameters are applied to the delay compensator to generate the next command based on the desired displacements, previous displacement responses, and/or commands. Three significant components, namely, the discrete loading system model, the delay compensator, and the parameter identification method, will be discussed herein.

2.1 Discrete model of a loading system

A model is used to establish the relationship between the commands and responses of the loading system that can be employed to predict the system output corresponding to specific commands and accommodate the influence of the system delay. The delay is an important characteristic of the loading system, and delay variations imply a model parameter change in the loading system. Consequently, the variable delay can be captured and compensated for by identifying the model parameters. The adaptation of delay compensation to system characteristic changes can be achieved in this manner. A discrete model of the loading system is chosen as

$$d_c^{i+1} = \sum_{j=1}^p d_c^{i-j+1} \cdot \theta_c^j + \sum_{k=1}^q d_m^{i-k+2} \cdot \theta_m^k \quad (1)$$

where d_c and d_m are the command and measured displacements of the loading system, respectively, and θ_c^j and θ_m^k are the respective model parameters relevant to the command and measured displacements, with p and q denoting the numbers of parameters/terms. For brevity, Eq. (1) can be re-expressed in a more compact form, namely

$$d_c^i = \varphi_i^T \theta \quad (2)$$

with

$$\begin{cases} \varphi_i^T = [d_c^i, \dots, d_c^{i-p+1}, d_m^{i+1}, d_m^i, \dots, d_m^{i-q+2}] \\ \theta = [\theta_c^i, \dots, \theta_c^p, \theta_m^1, \dots, \theta_m^q]^T \end{cases}$$

To establish this model, one first must determine the values of parameters p and q and further identify the values of parameters θ_c^j and θ_m^k with real testing data φ . The

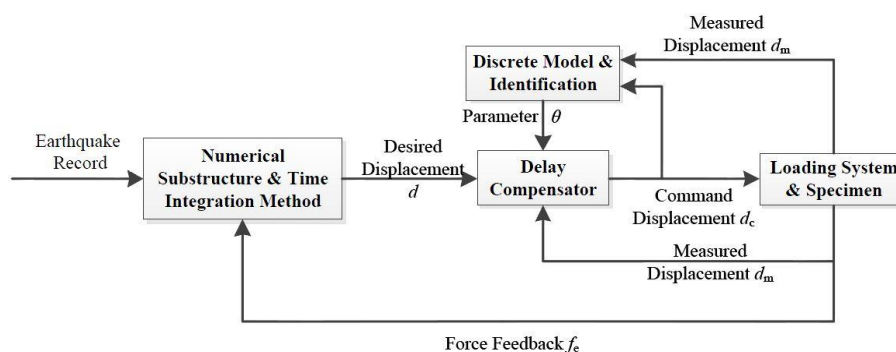


Fig. 1 Principle of adaptive delay compensation for RTHS

optimal numbers of parameters and the identification method for this adaptive delay compensation will be described in the following sections.

2.2 Parameter identification

This study used the least-squares method with a forgetting factor for parameter identification (Söderström and Stoica 1989). This method is very suitable for real-time applications owing to its small data storage size and low-computational cost. Additionally, the forgetting factor weakens the influence of older data on the estimated parameter values. Thus, this method can be applied to time-varying systems, e.g., a loading system with a varying delay. This method updates the parameters with

$$\begin{cases} \hat{\boldsymbol{\theta}}_i = \hat{\boldsymbol{\theta}}_{i-1} + \frac{\mathbf{P}_{i-1}\boldsymbol{\Phi}_1}{\lambda + \boldsymbol{\Phi}_i^T\mathbf{P}_{i-1}\boldsymbol{\Phi}_1} [d_c^i - \boldsymbol{\Phi}_i^T\hat{\boldsymbol{\theta}}_{i-1}] \\ \mathbf{P}_i = \frac{1}{\lambda} \left[\mathbf{I} - \frac{\mathbf{P}_{i-1}\boldsymbol{\Phi}_1}{\lambda + \boldsymbol{\Phi}_i^T\mathbf{P}_{i-1}\boldsymbol{\Phi}_1} \boldsymbol{\Phi}_i^T \right] \mathbf{P}_{i-1} \end{cases} \quad (3)$$

where λ denotes the forgetting factor such that $0.9 \leq \lambda \leq 1$, \mathbf{I} is an identity matrix with a size equal to the size of the parameter number, \mathbf{P}_i is the covariance matrix at the i -th step, and $\hat{\boldsymbol{\theta}}_i$ represents the identified parameters at the i -th step. The initial covariance \mathbf{P}_0 and parameter $\boldsymbol{\theta}_0$ are evaluated by the standard least-squares method with offline test data, namely

$$\begin{aligned} \hat{\boldsymbol{\theta}}_0 &= (\boldsymbol{\Phi}^T\boldsymbol{\Phi})^{-1}\boldsymbol{\Phi}^T\mathbf{Y} \\ \mathbf{P}_0 &= (\boldsymbol{\Phi}^T\boldsymbol{\Phi})^{-1} \end{aligned} \quad (4)$$

with

$$\begin{aligned} \boldsymbol{\Phi} &= [\boldsymbol{\Phi}_1, \boldsymbol{\Phi}_2 \dots \boldsymbol{\Phi}_L]^T \\ \mathbf{Y} &= [d_c^1, d_c^2 \dots d_c^L]^T \end{aligned}$$

where L indicates the length of the data. To obtain the offline test data, one can evaluate and impose the response of the NS on the specimen. This process is implemented in the validation test and presented in Section 4.

2.3 Delay compensator

This section explains how to compensate for the system delay and dynamics based on the identified model. With the assumption that the system parameters vary slowly, the identified parameters at the i -th step are considered a good approximation of $\boldsymbol{\theta}_{i+1}$, namely

$$\boldsymbol{\theta}_{i+1} \approx \hat{\boldsymbol{\theta}}_i \quad (5)$$

At this moment, d_m^{i+1} is unknown, and $d_c^i, d_c^{i-1}, \dots, d_c^{i-p+1}, d_m^i, d_m^{i-1}, \dots, d_m^{i-q+2}$ are known. In addition, the desired displacement d^{i+1} is provided by a time integration method, e.g., the central difference method. The objective of delay compensation is to reduce the error between the desired displacement and the actual measured displacement. Therefore, to generate the actuator command, one can replace the measured displacement d_m^{i+1} with d^{i+1} . Finally, the compensator is

$$d_c^{i+1} = \boldsymbol{\Phi}_{i+1}^T \hat{\boldsymbol{\theta}}_i \quad (6)$$

with

$$\boldsymbol{\Phi}_{i+1}^T = [d_c^i, \dots, d_c^{i-p+1}, d^{i+1}, d_m^i, \dots, d_m^{i-q+2}].$$

Obviously, if $\hat{\boldsymbol{\theta}}_i$ is sufficiently close to the real parameter $\boldsymbol{\theta}_{i+1}$, then the commands calculated by Eq. (6) can drive the actuator to obtain displacements close to the desired values. As a result, not only the system delay but also the system dynamics can be effectively compensated for.

The features of this method are as follows: (1) this method is solely dependent on the discrete displacement data rather than on the velocity and acceleration data and (2) the displacement commands generated by this method are evaluated with previous commands, previous measured displacements, and with the next desired displacement. Therefore, this method is more general than the existing methods, and is straightforward and suitable for implementation on digital signal processing boards.

2.4 Implementation procedure

Implementation of this studied method includes two phases, i.e., offline and online testing. Offline tests provide necessary data for initializing the recursive identification method and for assessing the performance of the method for prescribed desired displacement loading. Online tests refer to the actual RTHS. Therefore, the flowchart of RTHS, which uses this compensation method, is summarized as follows (Wang *et al.* 2018):

- Step 1: Evaluate the structural response with or without a specimen model.
- Step 2: Impose the structural response on the specimen, and measure the displacement response.
- Step 3: Determine the discrete model and identify parameters with the standard least-squares method listed in Eq. (4).
- Step 4: Determine the forgetting factor and set $i = 0$.
- Step 5: Evaluate the structural response at $(i+1)$ -th with the measured force.
- Step 6: Compute the actuator command using Eq. (6).
- Step 7: Send the command to the loading system.
- Step 8: Measure the reaction force and displacement response of the specimen at t_{i+1} .
- Step 9: Identify and update the model parameters using the least-squares method with the forgetting factor, as shown in Eq. (3).
- Step 10: For $i \leftarrow i + 1$, return to Step 5 until the test terminates.

3. Virtual RTHS

To evaluate this compensation method, various virtual RTHS are performed in this section by considering different discrete system models, measurement noise levels, and loading system characteristics.

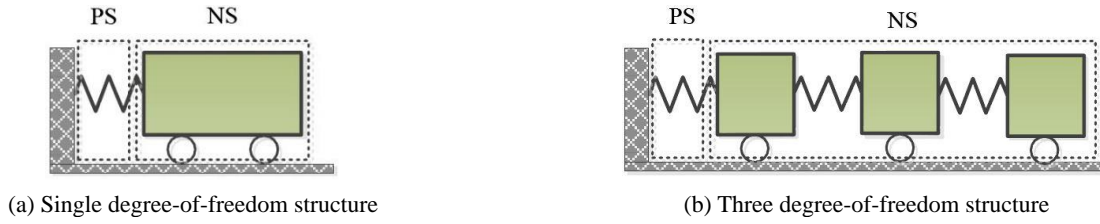


Fig. 2 Schematic of the emulated structures

3.1 Numerical model

Two emulated structures, i.e., one with single degree-of-freedom (SDOF) and another one with three degree-of-freedom (3DOF) as shown in Fig. 2, were performed virtual RTHS for verifying the effectiveness of the investigated method. In Fig. 2(a), the lumped mass and stiffness are respectively equal to 1000 kg and 39.4784 kN/m and thus lead to a natural frequency of 1 Hz. In Fig. 2(b), the masses and stiffnesses of the NS are respectively set to 1 kg and 200 kN/m, while the PS is assumed as a bilinear model with the initial stiffness of 200 kN/m, the yielding displacement of 0.006 m, and the second stiffness of 100 kN/m. The structural properties of the 3DOF structure are so determined that the initial structural frequencies equal to 1.0 Hz, 2.8 Hz, and 4.1 Hz, respectively. Additionally, Rayleigh damping is endowed to this 3DOF structure with a damping ratio of 0.02 for the first and second vibration modes. The El Centro earthquake (NS, 1940) record with a peak ground acceleration (PGA) tuned to 0.263 g was adopted to excite the structure. The equation of motion was discretized and solved by the central difference method with an integration time interval of 10/1024 s. Because there is no damping in the SDOF structure as shown in Fig. 2(a), any under-compensation or over-compensation for the delay causes high-amplitude errors in the structural response. That is to say, the simulation results are very sensitive to delay compensation performance. Note that the 3DOF structure model was adopted in Subsection 3.5 whereas all other analysis was carried out on the SDOF structure.

To determine the properties of this compensation method, herein, three different compensators were taken into account, as listed in Table 1. For comparison purposes, conventional polynomial extrapolation (PE) was also performed. Third-order PE was employed as follows

$$d_c^{i+1} = \left(1 + \frac{11}{6}\eta + \eta^2 + \frac{1}{6}\eta^3\right)d^{i+1} - \left(3\eta + \frac{3}{2}\eta^2 + \frac{1}{2}\eta^3\right)d^i + \left(\frac{3}{2}\eta + 2\eta^2 + \frac{1}{2}\eta^3\right)d^{i-1} \quad (7)$$

$$-\left(\frac{1}{3}\eta + \frac{1}{2}\eta^2 + \frac{1}{6}\eta^3\right)d^{i-2} \quad (7)$$

where $\eta = \frac{\tau}{\Delta t}$, and τ and Δt are the time delays of the loading system and the time interval, respectively. In the simulation, $\tau = 0.021$ s and $\Delta t = 10/1024$ s.

3.2 Performance indicators

To quantify the performances of different methods, four performance indicators are defined. The first indicator, J_1 , which is the maximum absolute synchronization error, is defined as the maximum value of the absolute error between the desired and measured displacements, i.e., $\max[\text{abs}(d_m - d)]$. Similarly, the maximum absolute experimental error J_2 denotes the maximum value of the absolute error between the desired and reference displacements, i.e., $\max[\text{abs}(d - d_r)]$. Additionally, the normalized root-mean-square error (NRMSE) is used to define the indicators J_3 and J_4 , which are formulated as

$$J_3 = \sqrt{\frac{\sum_{i=1}^N (d^i - d_m^i)^2}{\sum_{i=1}^N (d^i)^2}} \quad (8)$$

$$J_4 = \sqrt{\frac{\sum_{i=1}^N (d_r^i - d^i)^2}{\sum_{i=1}^N (d_r^i)^2}} \quad (9)$$

where d^i , d_m^i , and d_r^i denote the desired, measured, and reference displacements at the i -th step, respectively, and N represents the length of the data.

3.3 Simulation results for a time-invariant loading system

The simulations in this section are performed with a time-invariant loading system model, namely, a second-order transfer function, i.e.

$$T(s) = \frac{\omega^2}{s^2 + 2\zeta\omega s + \omega^2} \quad (10)$$

Table 1 Various discrete models and delay compensators

Model name	Discrete model of the loading system	Delay compensator
Two-parameter model	$d_c^{i+1} = \theta_m^1 d_m^{i+1} + \theta_m^2 d_m^i$	$d_c^{i+1} = \theta_m^1 d^{i+1} + \theta_m^2 d_m^i$
Three-parameter model	$d_c^{i+1} = \theta_m^1 d_m^{i+1} + \theta_m^2 d_m^i + \theta_m^3 d_m^{i-1}$	$d_c^{i+1} = \theta_m^1 d^{i+1} + \theta_m^2 d_m^i + \theta_m^3 d_m^{i-1}$
Four-parameter model	$d_c^{i+1} = \theta_c^1 d_c^{i-1} + \theta_m^1 d_m^{i+1} + \theta_m^2 d_m^i + \theta_m^3 d_m^{i-1}$	$d_c^{i+1} = \theta_c^1 d_c^{i-1} + \theta_m^1 d^{i+1} + \theta_m^2 d_m^i + \theta_m^3 d_m^{i-1}$

whereby the equivalent circular frequency $\omega = 50$ rad/s, and the damping ratio $\zeta = 0.80$. This is a second-order system that can be discretized and accurately expressed using the four-parameter model defined in Table 1. Two- and three-parameter models are adopted herein to evaluate the robustness of this method.

Fig. 3 illustrates the simulation results. From the global views, all the methods perform relatively well. From the close-up views, the studied methods, including the two-, three-, and four-parameter models, outperform the conventional PE method. Moreover, three different models of the studied method provide very consistent displacement values. In fact, the loading system in Eq. (10) discretized using a zero-order hold yields a model that can be accurately expressed using the four-parameter model. Thus, the discrete model is capable of accurately modeling the system, and an excellent compensation performance is thus expected. In the simulations, the two-parameter and three-parameter models perform as well as the four-parameter model, although theoretically, the models are not accurate enough to capture the characteristics of the loading system. The results demonstrate the excellent robustness of this method, thus indicating good performance, even with some modeling errors. Moreover, from the close-up views, one can observe that the results provided by the PE method have

amplitude and phase errors with respect to the reference values. These errors result from the delay compensation error, and can induce serious synchronization errors and NRMSE, as listed in Table 2.

The estimated parameters are depicted in Fig. 4. The parameters of the two-parameter model are relatively smooth during the entire simulation, while small fluctuations can be observed in the parameters of the three- and four-parameter models. These fluctuations are attributed to the fact that the latter two models are more sensitive to disturbances. Generally, these simulations show that three types of parameter models are adequate for modeling this loading system.

The indicator results are listed in Table 2. These results show that this method achieves very accurate compensation and that the conventional method achieves the worst compensation. In fact, the synchronization error J_1 of the conventional method is considerably smaller compared with the peak displacement of approximately 20 mm. The large error between the desired and reference displacements, J_2 , is attributed to the cumulative loading synchronization errors, i.e., the period elongation error due to delay compensation. This result reflects the necessity to perform adaptive delay compensation. Among the three models associated with this method, the four-parameter model performs best owing to

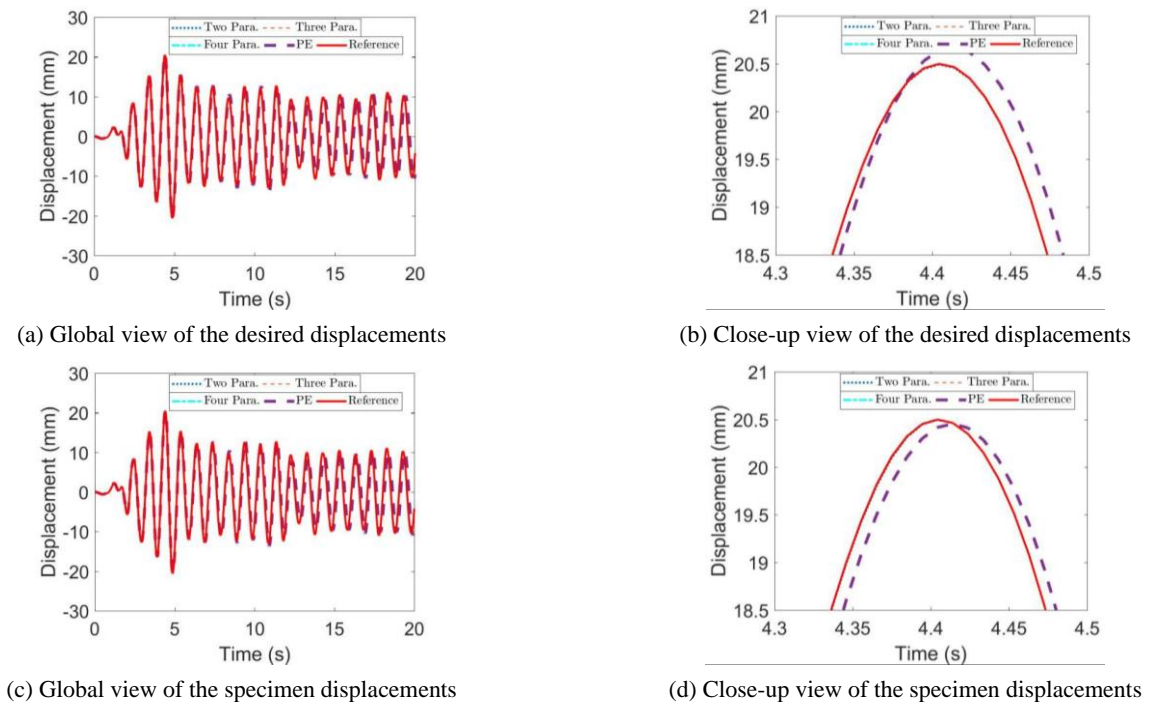


Fig. 3 Results of virtual RTHS with a time-invariant loading system

Table 2 Performance indicators for virtual RTHS for a time-invariant loading system

Compensator	J_1 (mm)	J_2 (mm)	J_3 (%)	J_4 (%)
PE	0.2651	6.5603	1.04	33.62
Two-parameter model	0.0149	0.0183	0.03	0.13
Three-parameter model	0.0129	0.0100	0.02	0.07
Four-parameter model	0.0072	0.0024	0.01	0.02

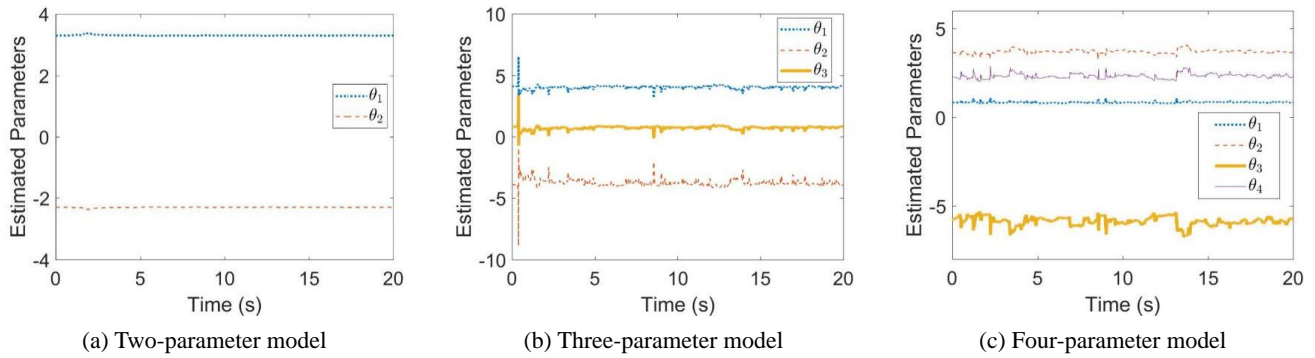


Fig. 4 Estimated parameters of various discrete models

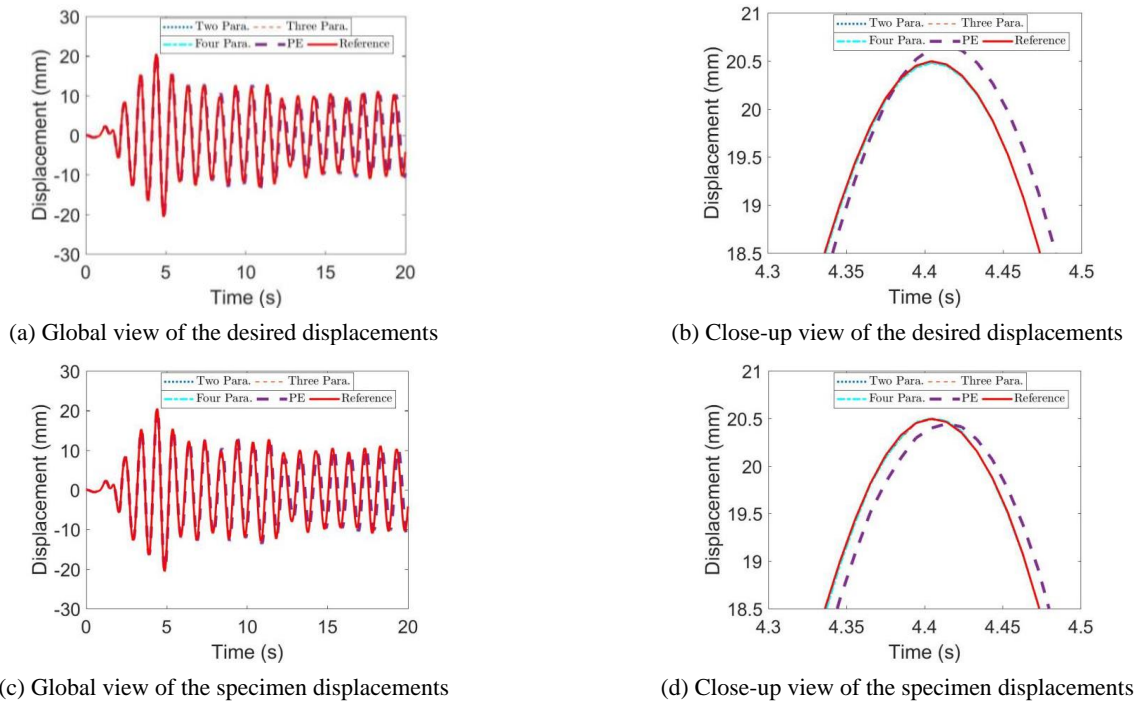


Fig. 5 Results of virtual RTHS with a time-invariant loading system and measurement noise

Table 3 Performance indicators for virtual RTHS with a time-invariant loading system and measurement noise

Compensator	J_1 (mm)	J_2 (mm)	J_3 (%)	J_4 (%)
PE	0.2727	6.5461	1.05	33.58
Two-parameter model	0.0324	0.0122	0.11	0.06
Three-parameter model	0.0478	0.0530	0.16	0.32
Four-parameter model	0.1973	0.0833	0.29	0.35

its excellent applicability to this loading system. The two-parameter model exhibits the largest error in its approximation of this loading system among the three models.

3.3 Simulation results for a time-invariant loading system considering measurement noise

High-frequency noise is inevitably introduced in the measured signals. Moreover, delay compensation often

results in that predicted signals are sensitive to system noise. To validate the performance of the studied method, the simulations in the previous subsection were repeated based on considerations of the measurement noise. The measured displacement d_m in this subsection includes white noise with a mean of zero and a standard variance of 0.01 mm.

The simulation results presented in Fig. 5 are consistent with those in the previous subsection, and the investigated method behaves well. From the indicators listed in Table 3,

the four-parameter model provides the worst results among the models of the studied method, and the two-parameter model yields the best performance, unlike in the previous case described in Table 2. Therefore, as the number of model parameters increases, the more sensitive the model becomes to measurement noise. Additionally, the PE method exhibits a minor difference from its counterpart (Table 2) because it is a pure forward prediction approach based on the desired displacements that are minimally affected by measurement noise. In summary, the low-order models of the studied method are more robust, accurate, and applicable in real tests compared to high-order models.

3.4 Simulation results for a time-varying loading system model considering measurement noise

Adaptive delay compensation aims to circumvent time-varying delays in RTHS. As a result, this subsection presents simulations with a time-varying loading system model and the measurement noise. For simplicity, the

system is modeled by Eq. (10) with a time-varying equivalent frequency. In particular, we assume that the model frequency changes sinusoidally, namely, $\omega = 50 + 5\sin(t)$ rad/s, which results in the system delay fluctuation by approximately 8 ms. Additionally, the same measurement noise is taken into account as in the previous subsection.

To identify the time-varying system parameters, a proper value of the forgetting factor must be chosen in the recursive least-squares method. A small forgetting factor decreases the impact of older data on the identified parameters, and is thus more suitable for time-varying systems. However, small forgetting factors may cause serious fluctuations in the identified parameters. To examine the generality of this method, the same forgetting factor (equal to 0.97) as that used in the previous sections is employed herein. Moreover, the same initial parameters are adopted.

The simulation results in Fig. 6 illustrate the performance of the studied method. Fig. 7 shows that the

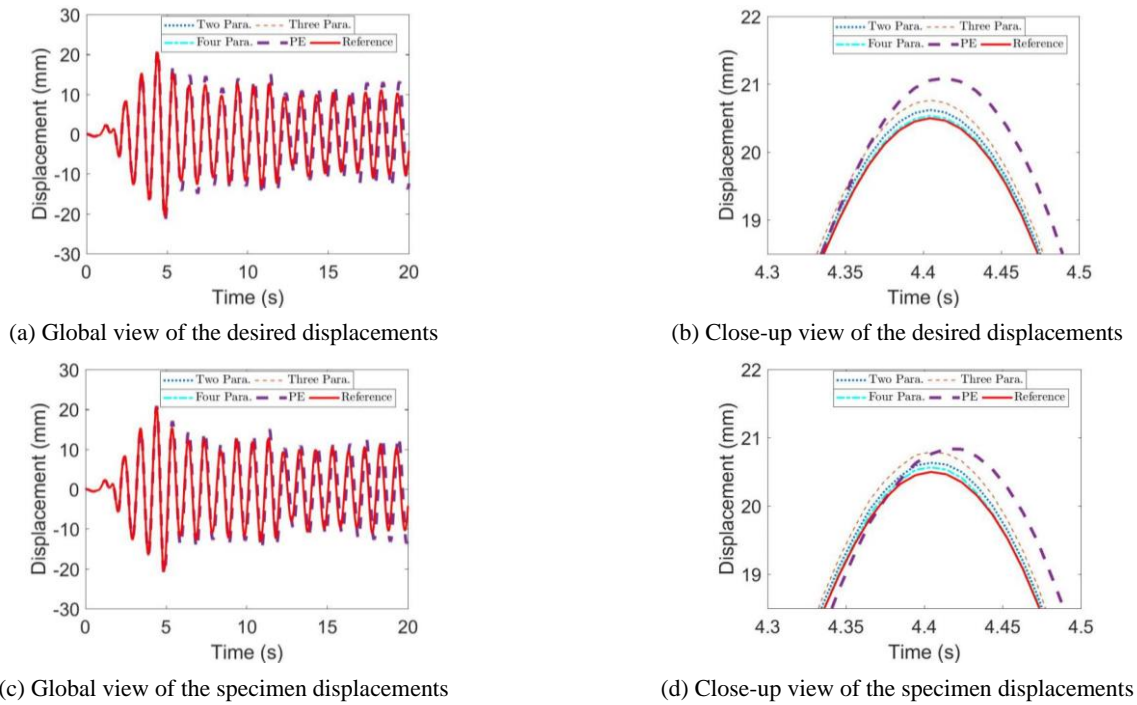


Fig. 6 Results of virtual RTHS with a time-varying loading system model considering measurement noise

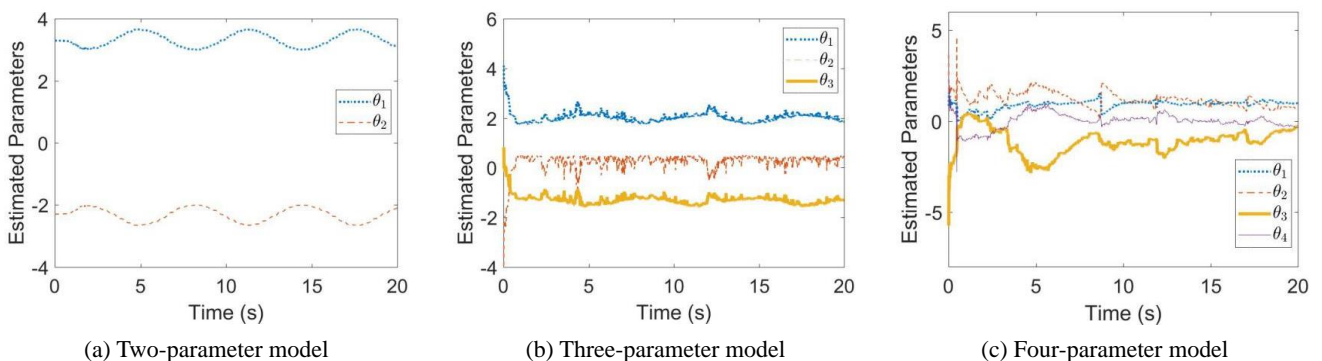


Fig. 7 Estimated parameters for various discrete models

Table 4 Performance indicators for virtual RTHS with a time-varying system model considering measurement noise

Compensator	J_1 (mm)	J_2 (mm)	J_3 (%)	J_4 (%)
Polynomial	0.6437	8.8620	1.91	43.68
Two-parameter model	0.0437	0.1469	0.18	0.76
Three-parameter model	0.0849	0.3017	0.34	1.51
Four-parameter model	0.3267	0.0866	0.32	0.43

identified parameters of the two-parameter model are smooth and vary with the equivalent frequency of the loading system. The parameters of the three- and four-parameter models converge to smaller values than those in the previous subsections and vary with the system frequency. The indicators in Table 4 show that the performances of all three models are satisfactory. Although the identified parameters of the four-parameter model

fluctuate, the relevant indicators are favorable. From the results of these three simulation scenarios, one can observe that low-order models are more robust and more applicable than the high-order models, although all three can be effectively adopted.

3.5 Simulation results for nonlinear 3DOF structure with a time-varying loading system model and measurement noise

Virtual RTHS were implemented on the nonlinear 3DOF structure depicted in Fig. 2(b) with the consideration of the time-varying loading system model and measurement noise employed in Subsection 3.4. Fig. 8 presents the hysteresis relation of the specimen obtained with two-parameter compensation method. Fig. 9 plots desired and specimen displacements obtained using various compensation methods. Obviously, all three adaptive compensation methods perform considerably well and outperform the conventional PE method. This is consistent with the conclusions obtained in the prior subsections. Moreover, the similar performance of these adaptive compensation methods is attributed to the less effect of compensation

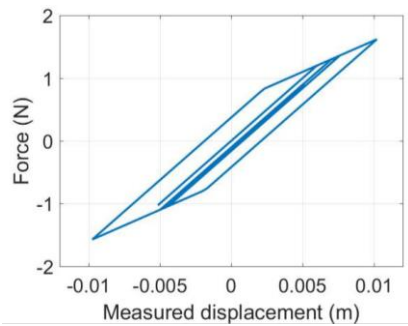
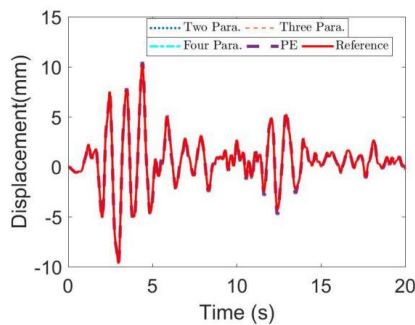
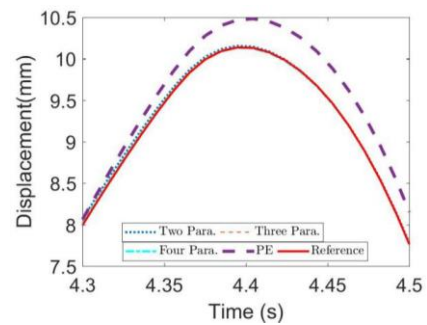


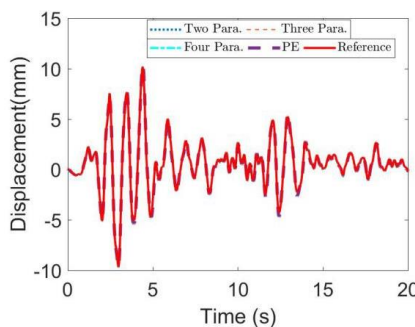
Fig. 8 Hysteresis relation of the specimen in the 3DOF structure



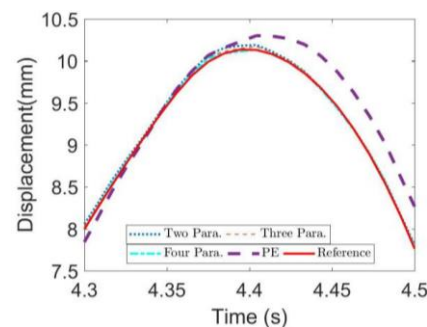
(a) Global view of the desired displacements



(b) Close-up view of the desired displacements

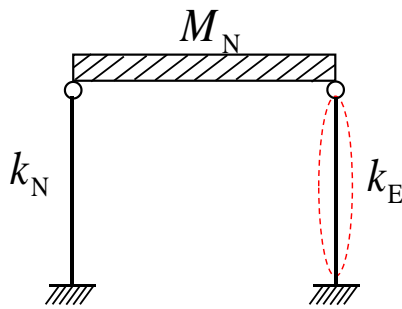


(c) Global view of the specimen displacements

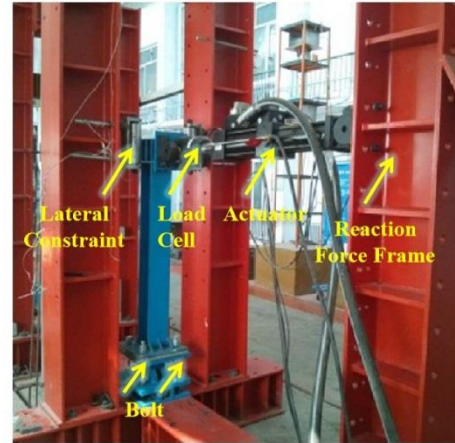


(d) Close-up view of the specimen displacements

Fig. 9 Results of virtual RTHS of 3DOF structure with a time-varying loading system model and measured noise



(a) Emulated structure



(b) Test setup

Fig. 10 Emulated structure and test setup

errors owing to the system damping and/or the dissipation of the specimen. This analysis indicates that the SDOF structure without damping is more beneficial for reflecting the compensation performance, and these adaptive methods are capable of dealing with time-varying delay in RTHS even with the consideration of measurement noise and specimen nonlinearity.

4. Validation tests

4.1 Characteristics of tests

A single degree-of-freedom system is used to validate the effectiveness of the investigated method, as shown in Fig. 10(a). The lumped mass and damping ratio of this structure are 500 kg and 5%, respectively. The right column is chosen as the test specimen, and the left column is modeled numerically with a stiffness k_N equal to 1.0 kN/mm. The specimen is shown in Fig. 10(b), whereby the main deformation occurs at the bolts at the bottom part of the column. The lateral stiffness k_E of the specimen was found to be 1.1 kN/mm in preliminary tests. To excite the structure, the El Centro earthquake (NS, 1940) record with a PGA of 0.1052 g was adopted. The actual RTHS was performed using an MTS loading system characterized by a loading capacity of 100 kN and a stroke of 250 mm at the Structural and Seismic Testing Center, Harbin Institute of Technology. In the tests, the NS and adaptive delay compensation method were modeled within Simulink and were operated in real-time with a dSpace card modeled by ds1104. The specimen was loaded with an MTS actuator that traced the commands generated by the card. The equation of motion of the structure was discretized and solved by the central difference method with a time interval of 10/1024 s.

4.2 Delay compensation for a prescribed desired displacement

Prior to RTHS, a loading test without/with delay compensation for the prescribed desired displacement is

often informative. First, a loading test without delay compensation can provide testing data from which the delay compensation parameter can be initialized. Second, a loading test with delay compensation can be adopted to examine the parameter estimation and compensation performance. In addition, because the reaction force of the physical substructure in this case is not fed back to the time integration algorithms, instabilities due to the loading delay will not occur. Therefore, the structural response was assessed without the considered specimen, and the response was then imposed on the specimen as the desired displacement in two different cases, i.e., without and with delay compensation. The two- and three-parameter models are employed herein owing to their favorable performance, as shown in the virtual RTHS.

The test results in Table 5 show that both models exhibit satisfactory performance. The two-parameter model leads to the indicators of $J_1 = 0.0546$ mm and $J_3 = 0.56\%$, and the three-parameter model indicators are $J_1 = 0.0773$ mm and $J_3 = 0.87\%$. Thus, the two models perform excellently in this real application. Notably, to save space, only the indicator results are presented herein, although further materials such as figures are also available.

4.3 Final RTHS

In the tests, safety has been considered thoroughly. To ensure the stability of the compensation, the stability criterion of the discrete system was checked. Specifically, it was ensured that the poles of the discrete transfer function were within a unit circle in the complex plane (Levine 1999). Moreover, the parameter estimation and updating schemes were suspended when the measured displacement

Table 5 Performance indicators for loading tests with a prescribed desired displacement

Compensator	J_1 (mm)	J_3 (%)
Two-parameter model	0.0546	0.56
Three-parameter model	0.0773	0.87

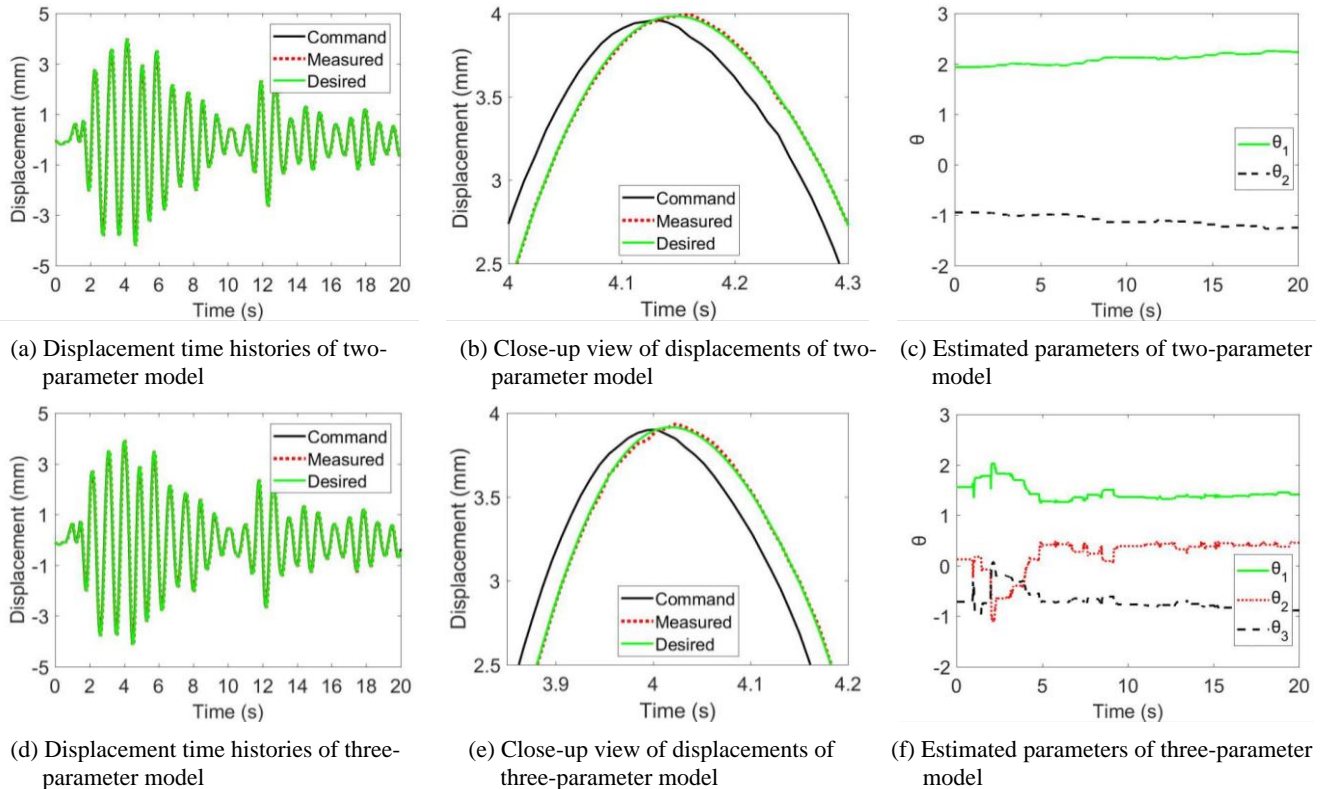


Fig. 11 Comparison of delay compensations in RTHS obtained with (a)–(c) the two-parameter model and (d)–(f) the three-parameter model

Table 6 Performance indicators used for real RTHS

Compensator	J_1 (mm)	J_3 (%)
Two-parameter model	0.04	0.71
Three-parameter model	0.1014	1.07

was less than 0.5 mm in instances at which the signal-to-noise value was low.

One can observe in Fig. 11 that the estimated parameters of the two-parameter model vary more slowly than those of the three-parameter model. This is consistent with the results obtained in previous simulations and the test results obtained using the prescribed desired displacements. The two close-up views demonstrate that the measured displacements with the two models match the desired displacements closely. As listed in Table 6, the maximum errors between the desired and measured displacements are 0.04 mm and 0.1014 mm, respectively, in the two cases. The two tests yielded NRMSE values equal to 0.71% and 1.07%. This finding shows that for this real application, the studied method exhibits outstanding performance, especially with the low-order model.

To depict the corresponding variation, the loading system delay is evaluated from the identified discrete models. As shown in Fig. 12, with the exception of the observed fluctuation at 2 s in the three-parameter model, the delays calculated using the two models match well. These findings indicate that both models successfully captured the dynamic characteristics of the loading system.

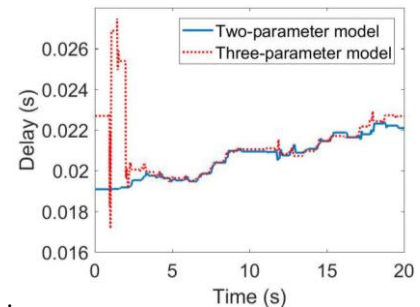


Fig. 12 Comparison of delays identified with the two- and three-parameter models

5. Conclusions

To resolve variable delay problems in RTHS, this study investigated an adaptive delay compensation method based on a discrete loading system model. Virtual and actual RTHS were performed to examine the performance of this method. The main conclusions drawn are as follows.

- The principle of the studied adaptive delay compensation method for RTHS was presented. This method employs a discrete model with parameters that are online identified and updated with the least-squares method to represent a servo hydraulic loading system. Based on this model, the system delay is compensated for by generating system commands using the desired displacements,

achieved displacements, and previous displacement commands. This method is more general than existing compensation methods because it generates commands based on multi-category displacements. Moreover, this method is more straightforward and suitable for the implementation on digital signal processing boards than traditional methods.

- Virtual RTHS were conducted to evaluate the effectiveness of the investigated method based on considerations of a time-invariant/time-varying loading system with/without noise. The numerical results showed that this method achieved excellent smoothness for the identified parameters and increased accuracy in delay compensation. The two-parameter model displayed better robustness than the high-order models in RTHS in the presence of measurement noise. Moreover, the investigated method exhibited superior delay compensation performance compared to the polynomial extrapolation method for the time-varying loading system.
- Actual experimental verifications of RTHS were performed to validate the effectiveness of the studied method with two- and three-parameter models. The experimental results demonstrated that this method with two- and three-parameter models performed well in real applications, and that the low-order model, i.e., the two-parameter model, displayed better robustness than the high-order model.

One should note that this study provides a high-performance delay compensation method for the RTHS of civil engineering structures, and the frequencies of the desired displacements are normally less than 10 Hz. It is necessary to further investigate the effectiveness of the studied method for RTHS of structures with higher dominant frequencies.

Acknowledgments

The authors gratefully acknowledge the financial support from the National Key Research and Development Program of China (Grant Nos. 2017YFC0703605 and 2016YFC0701106) and the National Natural Science Foundation of China (Grant Nos. 51978213, 51878525, 51778190, and 51408157).

References

- Ahmadzadeh, M., Mosqueda, G. and Reinhorn, A.M. (2008), "Compensation of actuator delay and dynamics for real-time hybrid structural simulation", *Earthq. Eng. Struct.*, **37**(1), 21-42. <https://doi.org/10.1002/eqe.743>
- Bonnet, P., Lim, C., Williams, M., Blakeborough, A., Neild, S., Stoten, D. and Taylor, C. (2007), "Real-time hybrid experiments with newmark integration, MCSmd outer-loop control and multi-tasking strategies", *Earthq. Eng. Struct. Dyn.*, **36**(1), 119-141. <https://doi.org/10.1002/eqe.628>
- Chae, Y., Kazemibidokhti, K. and Ricles, J.M. (2013), "Adaptive time series compensator for delay compensation of servo-

- hydraulic actuator systems for real-time hybrid simulation", *Earthq. Eng. Struct. Dyn.*, **42**(11), 1697-1715. <https://doi.org/10.1002/eqe.2294>
- Chae, Y., Ricles, J.M. and Sause, R. (2014), "Large-scale real-time hybrid simulation of a three-story steel frame building with magneto-rheological dampers", *Earthq. Eng. Struct. Dyn.*, **43**(13), 1915-1933. <https://doi.org/10.1002/eqe.2429>
- Chae, Y., Park, M., Kim, C.Y. and Park, Y.S. (2017), "Experimental study on the rate-dependency of reinforced concrete structures using slow and real-time hybrid simulations", *Eng. Struct.*, **132**, 648-658. <https://doi.org/10.1016/j.engstruct.2016.11.065>
- Chen, C. and Ricles, J. (2009), "Improving the inverse compensation method for real-time hybrid simulation through a dual compensation scheme", *Earthq. Eng. Struct. Dyn.*, **38**(10), 1237-1255. <https://doi.org/10.1002/eqe.904>
- Chen, C., Ricles, J.M. and Guo, T. (2012), "Improved adaptive inverse compensation technique for real-time hybrid simulation", *J. Eng. Mech.*, **138**(12), 1432-1446. [https://doi.org/10.1061/\(ASCE\)EM.1943-7889.0000450](https://doi.org/10.1061/(ASCE)EM.1943-7889.0000450)
- Chen, P.C., Hsu, S.C., Zhong, Y.J. and Wang, S.J. (2019), "Real-time hybrid simulation of smart base-isolated raised floor systems for high-tech industry", *Smart Struct. Syst., Int. J.*, **23**(1), 91-106. <https://doi.org/10.12989/sss.2019.23.1.091>
- Christenson, R. and Lin, Y. (2008), "Real-time hybrid simulation of a seismically excited structure with large-scale magneto-rheological fluid dampers", In: *Hybrid Simulation: Theory, Implementation and Applications*, (V. Saouma and M. Sivaselvan eds.), Taylor & Francis, pp. 169-180.
- Darby, A.P., Williams, M.S. and Blakeborough, A. (2002), "Stability and delay compensation for real-time substructure testing", *J. Eng. Mech.*, **128**(12), 1276-1284. [https://doi.org/10.1061/\(ASCE\)0733-9399\(2002\)128:12\(1276\)](https://doi.org/10.1061/(ASCE)0733-9399(2002)128:12(1276))
- Eem, S.H., Koo, J.H. and Jung, H.J. (2018), "Feasibility study of an adaptive mount system based on magnetorheological elastomer using real-time hybrid simulation", *J. Intell. Mater. Syst. Struct.*, 1045389X1875434. <https://doi.org/10.1177/1045389X18754347>
- Gao, X., Castaneda, N. and Dyke, S.J. (2013), "Real time hybrid simulation: from dynamic system, motion control to experimental error", *Earthq. Eng. Struct. Dyn.*, **42**(6), 815-832. <https://doi.org/10.1002/eqe.2246>
- Hayati, S. and Song, W. (2017), "An optimal discrete-time feedforward compensator for real-time hybrid simulation", *Smart Struct. Syst., Int. J.*, **20**(4), 483-498. <https://doi.org/10.12989/sss.2017.20.4.483>
- Horiuchi, T. and Konno, T. (2001), "A new method for compensating actuator delay in realtime hybrid experiments", *Philosophical Transactions of the Royal Society of London. Series A: Mathematical, Physical and Engineering Sciences*, **359**(1786), 1893-1909. <https://doi.org/10.1098/rsta.2001.0878>
- Horiuchi, T., Inoue, M., Konno, T. and Namita, Y. (1999), "Real-time hybrid experimental system with actuator delay compensation and its application to a piping system with energy absorber", *Earthq. Eng. Struct. Dyn.*, **28**(10), 1121-1141. [https://doi.org/10.1002/\(SICI\)1096-9845\(199910\)28:10<1121::AID-EQE858>3.0.CO;2-O](https://doi.org/10.1002/(SICI)1096-9845(199910)28:10<1121::AID-EQE858>3.0.CO;2-O)
- Huang, L., Chen, C., Guo, T. and Chen, M. (2019), "Stability analysis of real-time hybrid simulation for time-varying actuator delay using the lyapunov-krasovskii functional approach", *J. Eng. Mech.*, **145**(1), 04018124. [https://doi.org/10.1061/\(ASCE\)EM.1943-7889.0001550](https://doi.org/10.1061/(ASCE)EM.1943-7889.0001550)
- Jung, R. and Shing, P. (2006), "Performance evaluation of a real-time pseudo dynamic test system", *Earthq. Eng. Struct. Dyn.*, **35**(7), 789-810. <https://doi.org/10.1002/eqe.547>
- Levine, W.S. (1999), *Control System Fundamentals*, CRC Press, Boca Raton, FL, USA.

- Lu, L., Fernandois, G.A., Lu, X., Spencer, B.F. Jr., Duan, Y.F. and Zhou, Y. (2019), "Experimental evaluation of an inertial mass damper and its analytical model for cable vibration mitigation", *Smart Struct. Syst., Int. J.*, **23**(6), 589-613. <https://doi.org/10.12989/sss.2019.23.6.589>
- Nakashima, M. and Masaoka, N. (1999), "Real-time on-line test for MDOF systems", *Earthq. Eng. Struct. Dyn.*, **28**(4), 393-420. [https://doi.org/10.1002/\(SICI\)1096-9845\(199904\)28:4<393::AID-EQE823>3.0.CO;2-C](https://doi.org/10.1002/(SICI)1096-9845(199904)28:4<393::AID-EQE823>3.0.CO;2-C)
- Nakashima, M., Kato, H. and Takaoka, E. (1992), "Development of real-time pseudo dynamic testing", *Earthq. Eng. Struct. Dyn.*, **21**(1), 79-92. <https://doi.org/10.1002/eqe.4290210106>
- Ning, X., Wang, Z., Zhou, H., Wu, B., Ding, Y. and Bin, X. (2019), "Robust actuator dynamics compensation method for real-time hybrid simulation", *Mech. Syst. Signal Process.*, **133**(15), 49-70. <https://doi.org/10.1016/j.ymsp.2019.05.038>
- Ou, G., Ozdagli, A.I., Dyke, S.J. and Wu, B. (2015), "Robust integrated actuator control: experimental verification and real-time hybrid-simulation implementation", *Earthq. Eng. Struct. Dyn.*, **44**(3), 441-460. <https://doi.org/10.1002/eqe.2479>
- Phillips, B.M. and Spencer, B.F. (2013), "Model-based feedforward-feedback actuator control for real-time hybrid simulation", *J. Struct. Eng.*, **139**(7), 1205-1214. [https://doi.org/10.1061/\(ASCE\)ST.1943-541X.0000606](https://doi.org/10.1061/(ASCE)ST.1943-541X.0000606)
- Shao, X., van de Lindt, J., Bahmani, P., Pang, W., Ziaei, E., Symans, M., Tian, J. and Dao, T. (2014), "Real-time hybrid simulation of a multi-story wood shear wall with first-story experimental substructure incorporating a rate-dependent seismic energy dissipation device", *Smart Struct. Syst., Int. J.*, **14**(6), 1031-1054. <https://doi.org/10.12989/sss.2014.14.6.1031>
- Söderström, T. and Stoica, P. (1989), *System Identification*, Prentice Hall.
- Strano, S. and Terzo, M. (2016), "Actuator dynamics compensation for real-time hybrid simulation: an adaptive approach by means of a nonlinear estimator", *Nonlinear Dyn.*, **85**(4), 2353-2368. <http://doi:10.1007/s11071-016-2831-0>
- Wallace, M., Sieber, J., Neild, S., Wagg, D. and Krauskopf, B. (2005a), "Stability analysis of realtime dynamic substructuring using delay differential equation models", *Earthq. Eng. Struct. Dyn.*, **34**(15), 1817-1832. <https://doi.org/10.1002/eqe.513>
- Wallace, M., Wagg, D. and Neild, S. (2005b), "An adaptive polynomial based forward prediction algorithm for multi-actuator real-time dynamic substructuring", *Proc. R. Soc.*, **461**(2064), 3807-3826. <https://doi.org/10.1098/rspa.2005.1532>
- Wang, Z., Wu, B., Bursi, O.S., Xu, G. and Ding, Y. (2014), "An effective online delay estimation method based on a simplified physical system model for real-time hybrid simulation", *Smart Struct. Syst., Int. J.*, **14**(6), 1247-1267. <http://doi:10.12989/sss.2014.14.6.1247>
- Wang, J.T., Gui, Y., Zhu, F., Jin, F. and Zhou, M.X. (2016), "Real-time hybrid simulation of multi-story structures installed with tuned liquid damper", *Struct. Control Heal. Monit.*, **23**(7), 1015-1031. <https://doi.org/10.1002/stc.1822>
- Wang, Z., Li, Q. and Wu, B. (2018), "Adaptive delay compensation method for real-time hybrid testing", *Eng. Mech.*, **35**(9), 37-43. [In Chinese]
- Wu, B. and Zhou, H. (2014), "Sliding mode for equivalent force control in real-time substructure testing", *Struct. Control Heal. Monit.*, **21**(10), 1284-1303. <https://doi.org/10.1002/stc.1648>
- Wu, B., Shi, P., Wang, Q., Guan, X. and Ou, J. (2011), "Performance of an offshore platform with MR dampers subjected to ice and earthquake", *Struct. Control Heal. Monit.*, **18**(6), 682-697. <https://doi.org/10.1002/stc.398>
- Wu, B., Wang, Z. and Bursi, O.S. (2013), "Actuator dynamics compensation based on upper bound delay for real-time hybrid simulation", *Earthq. Eng. Struct. Dyn.*, **42**(12), 1749-1765. <https://doi.org/10.1002/eqe.2296>
- Zhang, Z., Basu, B. and Nielsen, S.R.K. (2019), "Real-time hybrid aeroelastic simulation of wind turbines with various types of full-scale tuned liquid dampers", *Wind Energy.*, **22**(2), 239-256. <https://doi.org/10.1002/we.2281>
- Zhao, J., French, C., Shield, C. and Posbergh, T. (2003), "Considerations for the development of real-time dynamic testing using servo-hydraulic actuation", *Earthq. Eng. Struct. Dyn.*, **32**(11), 1773-1794. <https://doi.org/10.1002/eqe.301>
- Zhou, H., Wagg, D.J. and Li, M. (2017), "Equivalent force control combined with adaptive polynomial-based forward prediction for real-time hybrid simulation", *Struct. Control Heal. Monit.*, **24**(11), e2018. <https://doi.org/10.1002/stc.2018>

BS